

# Dynamic Behaviour of Plates Subjected to a Flowing Fluid

Y. KERBOUA AND A.A. LAKIS

Mechanical Engineering Department

École Polytechnique of Montreal

C.P. 6079, Succursale Centre-ville, Montreal, Quebec, H3C 3A7,

CANADA

aouni.lakis@polymtl.ca

*Abstract:* - Elastic structures subjected to a flowing fluid undergo a considerable change in their dynamic behaviour and can lose their stability. In this article we describe the development of a fluid-solid finite element to model plates subjected to flowing fluid under various boundary conditions. The mathematical model for the structure is developed using a combination of a hybrid finite element method and Sanders' shell theory. The membrane displacement field is approximated by bilinear polynomials and the transversal displacement by an exponential function. Fluid pressure is expressed by inertial, Coriolis and centrifugal fluid forces, written respectively as function of acceleration, velocity and transversal displacement. Bernoulli's equation for the fluid-solid interface and a partial differential equation of potential flow are applied to calculate the fluid pressure. The impermeability condition ensures contact between the system of plates and the fluid. Mass and rigidity matrices for each element are calculated by exact integration. Calculated results are in reasonable agreement with other analytical theories.

*Key-Words:* - Vibration, Finite element, Plates, Potential flow, Fluid structure interaction, Critical velocity.

## 1 Introduction

Systems of plates subjected to fluid flow are often found in contemporary industries such as nuclear reactors and aerospace. Generally these industries require high rates of fluid flow and low plate thicknesses. Under these conditions, if the length of the plates is excessive the structure becomes very susceptible to failure.

Earlier works in this field were carried out on engineering test reactor (ETR) systems consisting of many thin plates stacked in parallel with narrow channels between the plates to let coolant flow through. Miller [13] was the first to present a theoretical analysis predicting the critical flow velocity for divergence. His analysis applies a method of 'neutral equilibrium' whereby pressure and plate restoring forces are balanced, leading to a derivation of critical velocity of flow for various types of support. It is important to underline that the motion of a plate excited by fluid flow displaces the nearby fluid, and then the fluid reactive motion may further deform the plate. Excessive fluid reactive motion at a certain flow velocity over the surface of the plate is referred to as the divergent velocity, which may also be considered a critical flow velocity [8]. Rosenberg and Youngdahl [14] have formulated a dynamic model describing the motion

of a fuel plate in a parallel plate assembly. They found that good agreement exists between the results of the dynamic model and that of the neutral equilibrium used by Miller [13]. Three parallel plate assemblies were tested by Groninger and Kane [2] to investigate the flow-induced deflections of the individual plates. The model showed that adjacent plates always move in opposite directions at high flow rates, causing alternate opening and closing of the channel. They detected a violent dynamic instability at 1.9 times Miller's collapse velocity.

The assumptions of Miller [13], and Rosenberg and Youngdahl [14] were the same. They linearized the pressure drop expression using only a first-order approximation. Wambsganss [19] retained the second-order terms in an attempt to assess their influence on stability. The second-order terms generate an additional stability criterion in the form of an upper bound on the amplitude of quasi-static deflections for stable oscillations. He derived a new expression for critical velocity. Smislaert [17 and 18] performed analytical and experimental investigations on an MTR-type flat-plate fuel element. The experimental results [17] show that for low velocities the plates will deform as a result of static pressure differences in the channels between these plates. At high fluid velocities a high-

amplitude flutter vibration is observed. This flutter does not appear below a minimum average water velocity referred to as the flutter velocity, which is approximately equal to two times the Miller velocity of the assembly. In the analytical study, Smissaert [18] indicated that a plate assembly is characterized by two velocities; Miller's velocity and flutter velocity. One explanation of the dynamic instability is that the exciting frequency of the fully-developed turbulent flow approaches the in-fluid natural frequency of the plate. Theoretically, under this condition the amplitude of the plate vibration becomes large. Weaver and Unny [20] studied the dynamic behaviour of a single flat plate, one side of which is exposed to high flow velocity of a heavy fluid such as water. They examined the variation of natural frequencies according to the rate of flow. They concluded that for a given mass rapport, the neutral zone of stability is followed by a zone of static instability. After this stage the plate quickly returns to neutral stability, which continues until the occurrence of dynamic instability. Kornecki et al. [9] considered a flat panel of infinite width and finite length embedded in an infinite rigid plane with uniform incompressible potential flow over its upper surface. The studied plates were constrained (clamped or simply supported) along their leading and trailing edges. The case of a panel clamped at its leading edge and free at its trailing edge was investigated both theoretically and experimentally. The obtained results demonstrate that a panel fixed at its leading and trailing edges loses its stability by divergence (static instability), while the cantilevered panel loses its stability by flutter. Other investigators have studied the fluid flow effect on dynamic behaviour of rectangular plates; i.e. Ishii [6], Dowell [1] and Holmes [5]. More recently, Kim and Davis [8] developed an analytical model of a system of thin rectangular flat plates. Their model was used to investigate static and dynamic instabilities of the system. Guo and Paidoussis [3] studied theoretically the stability of rectangular plates with free side-edges in inviscid channel flow. They treated the plate as one dimensional and the channel flow as two-dimensional. The Galerkin method was employed to solve the plate equation, while the Fourier transform technique was employed to obtain the perturbation pressure from the potential flow equations. They investigated every possible combination of classical supports at the leading and trailing edges of the plates. They concluded that divergence and coupled mode flutter may occur for plates with any type of end supports,

while single mode flutter only arises for non-symmetrically supported plates. Guo and Paidoussis [4] have also conducted a theoretical study of the hydro-elastic instabilities of rectangular parallel-plate assemblies. They considered the plates as two-dimensional, with a finite length, and the flow field was assumed to be inviscid and three-dimensional. Two types of instability were found; single-mode flutter and coupled-mode flutter. They also concluded that the frequency at a given flow velocity decreases as the aspect ratio increases and the channel height to plate-width ratio decreases.

The purpose of this paper is to develop a solid-fluid finite element to study the dynamic response of a rectangular plate subjected to potential flow. This new finite element permits us to obtain the low as well as the high frequencies of fluid-structure systems with precision for any combination of boundary conditions without changing the displacement field. This finite element is applied to simulate a number of plates and set of parallel plates subjected to flowing fluid. The mathematical model for the structure is developed using a combination of the finite element method and Sanders' shell theory. The velocity potential and Bernoulli's equation are adopted to express the fluid pressure acting on the structure.

## 2 Solid finite element

The geometry of the mean surface of the rectangular plate and the co-ordinate systems used for this analysis are shown in Fig. 1.b. A typical four-node element and nodal degrees of freedom are shown in Fig. 1.a. Each node has six degrees of freedom consisting of in-plane and out-of-plane displacement components and their spatial derivatives.

### 2.1 Equilibrium equations and displacement functions

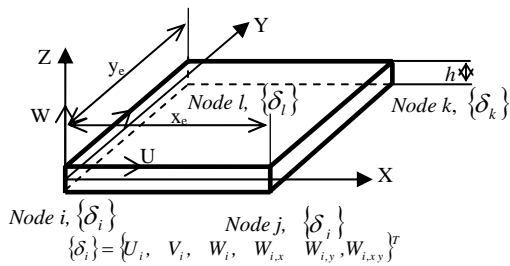
To develop the equilibrium equations for rectangular plates, the Sanders' equations for cylindrical shells are used assuming the radius to be infinite,  $\theta=y$  and  $rd\theta =dy$ . Both membrane and bending effects are taken into account in this theory. It is worthy to note that Sanders' shell theory is based on Love's first approximation theory but leads to zero strains for the case of rigid body motion. The developed displacement functions therefore satisfy the convergence criteria for the proposed finite element.

The equilibrium equations of a rectangular plate according to Sanders' theory can be written as a function of displacement components with respect to the reference surface:

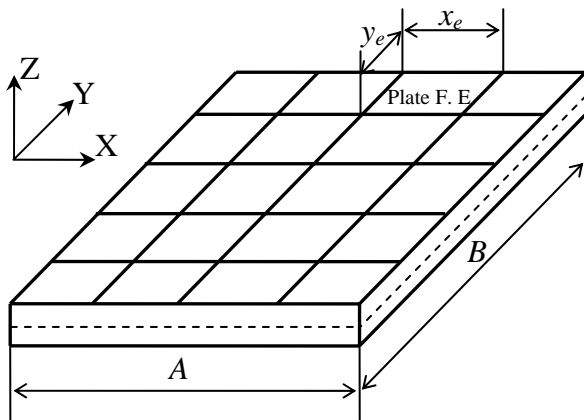
$$P_{22} \frac{\partial^2 V}{\partial y^2} + P_{21} \frac{\partial^2 U}{\partial x \partial y} + P_{33} \left( \frac{\partial^2 U}{\partial x \partial y} + \frac{\partial^2 V}{\partial x^2} \right) = 0 \quad (1.a)$$

$$P_{11} \frac{\partial^2 U}{\partial x^2} + P_{12} \frac{\partial^2 V}{\partial x \partial y} + P_{33} \left( \frac{\partial^2 V}{\partial x \partial y} + \frac{\partial^2 U}{\partial y^2} \right) = 0 \quad (1.b)$$

$$P_{44} \frac{\partial^4 W}{\partial x^4} + (P_{45} + P_{54} + 2P_{66}) \frac{\partial^4 W}{\partial x^2 \partial y^2} + P_{55} \frac{\partial^4 W}{\partial y^4} = 0 \quad (1.c)$$



(a)



(b)

Fig. 1: (a) Geometry and displacement field of a typical element, (b) Finite element discretization of a rectangular plate

Note that both circumferential and longitudinal hybrid elements used in the dynamic analysis of vertical Lakis and Paidoussis [22] and horizontal Lakis and Selmane [23] open cylindrical shells were developed based on exact solution of the equilibrium equations. This approach resulted in a very precise element which leads to fast convergence and less numerical difficulties from the computational point of view. This encouraged us to develop a new finite element using the same approach for dynamic analysis of rectangular plates.

Generally, exact solution of the equilibrium equations for the case of rectangular plates is difficult. To overcome this we present the in-plane membrane displacement components in terms of bilinear polynomials and the out-of-plane bending displacement component by an exponential function. Hence, the displacement field may be defined as follows:

$$U(x, y, t) = C_1 + C_2 \frac{x}{A} + C_3 \frac{y}{B} + C_4 \frac{xy}{AB} \quad (2.a)$$

$$V(x, y, t) = C_5 + C_6 \frac{x}{A} + C_7 \frac{y}{B} + C_8 \frac{xy}{AB} \quad (2.b)$$

$$W(x, y, t) = \sum_{j=9}^{24} C_j e^{i\pi \left( \frac{x}{A} + \frac{y}{B} \right)} e^{i\omega t} \quad (2.c)$$

where  $U$  and  $V$  represent the in-plane displacement components of the middle surface in  $X$  and  $Y$  directions, respectively,  $W$  is the transversal displacement of the middle surface,  $A$  and  $B$  are the plate dimensions in  $X$  and  $Y$  directions, " $\omega$ " is the natural frequency of the plate (rad/sec), " $i$ " is a complex number and  $C_j$  are unknown constants.

Equation (1.c) can be developed in Taylor's series as follows:

$$\begin{aligned} W(x, y, t) = & C_9 + C_{10} \frac{x}{A} + C_{11} \frac{y}{B} + C_{12} \frac{x^2}{2A^2} + C_{13} \frac{xy}{AB} + \\ & C_{14} \frac{y^2}{2B^2} + C_{15} \frac{x^3}{6A^3} + C_{16} \frac{x^2 y}{2A^2 B} + C_{17} \frac{xy^2}{2AB^2} + C_{18} \frac{y^3}{6B^3} + (3) \\ & C_{19} \frac{x^3 y}{6A^3 B} + C_{20} \frac{x^2 y^2}{4A^2 B^2} + C_{21} \frac{xy^3}{6AB^3} + C_{22} \frac{x^3 y^2}{12A^3 B^2} + \\ & C_{23} \frac{x^2 y^3}{12A^2 B^3} + C_{24} \frac{x^3 y^3}{36A^3 B^3} \end{aligned}$$

We can write the displacements  $U$ ,  $V$  and  $W$  in matrix form:

$$\begin{Bmatrix} U \\ V \\ W \end{Bmatrix} = [R] \{C\} \quad (4)$$

where  $[R]$  is a matrix of order  $(3 \times 24)$  in which the components are the  $x$  and  $y$  terms of Equations (2.a, 2.b and 3) without the unknown constants (see Appendix) and  $\{C\}$  is the vector for the unknown constants.

The components of this last vector can be determined using twenty-four degrees of freedom for a plate element as shown in Fig. 1. The displacement vector of each element is given as:

$$\{\delta\} = \left\{ \left\{ \delta_i \right\}^T, \left\{ \delta_j \right\}^T, \left\{ \delta_k \right\}^T, \left\{ \delta_l \right\}^T \right\}^T \quad (5)$$

Each node, i.e. "node  $i$ ", possesses a nodal displacement vector composed of the following terms:

$$\{\delta_i\} = \{U_i, V_i, W_i, \partial W_i / \partial x, \partial W_i / \partial y, \partial^2 W_i / (\partial x \partial y)\}^T \quad (6)$$

where  $U_i$  and  $V_i$  are nodal in-plane displacement components and  $W_i$  represent the nodal displacement components normal to the middle surface as shown in Fig. 1.a.

By introducing Equations (2.a, 2.b and 3) into relation (5), the elementary displacement vector can be defined as:

$$\{\delta\} = [A]\{C\} \quad (7)$$

The vector  $\{C\}$  in Equation (7) will be then replaced by the generalized displacement vector of a quadrilateral finite element. The displacement field may be described by the following relation:

$$\begin{Bmatrix} U \\ V \\ W \end{Bmatrix} = [R][A]^{-1}\{\delta\} = [N]\{\delta\} \quad (8)$$

where matrix  $[N]$  of order  $(3 \times 24)$  is the displacement shape function of the finite element and the terms of matrix  $[A]^{-1}$  are given in the Appendix.

### 2.2 Kinematics Relations

Strain-displacement relations for the rectangular plates are given as Sanders [15]:

$$\begin{Bmatrix} \varepsilon_x \\ \varepsilon_y \\ 2\varepsilon_{xy} \\ \kappa_x \\ \kappa_y \\ \kappa_{xy} \end{Bmatrix} = \begin{Bmatrix} \partial U / \partial x \\ \partial V / \partial y \\ \partial V / \partial x + \partial U / \partial y \\ -\partial^2 W / \partial x^2 \\ -\partial^2 W / \partial y^2 \\ -2\partial^2 W / (\partial x \partial y) \end{Bmatrix} \quad (9)$$

Substituting the displacement components defined in Equation (8) into the strain-displacement relationship (9), one obtains an expression for the strain vector as a function of nodal displacements.

$$\{\varepsilon\} = [Q][A]^{-1}\{\delta\} = [B]\{\delta\} \quad (10)$$

where matrix  $[Q]$  of order  $(6 \times 24)$  is given in the Appendix.

### 2.3 Constitutive Equations

The stress-strain relationship of an isotropic rectangular plate is defined as follows:

$$\{\sigma\} = [P]\{\varepsilon\} \quad (11)$$

where  $[P]$  is the elasticity matrix for an isotropic plate and no bending-membrane coupling is present (see Appendix). Substituting Equation (10) into

Equation (11) results in the following expression for the stress tensor:

$$\{\sigma\} = [P][B]\{\delta\} \quad (12)$$

The mass and stiffness matrices for one finite element can be expressed as:

$$[k_s]^e = \iint_S [B]^T [P] [B] dS \quad (13.a)$$

$$[m_s]^e = \rho_s h \iint_S [N]^T [N] dS \quad (13.b)$$

where  $S$  is the element surface area,  $h$  is the plate thickness,  $\rho_s$  is the material density and  $[P]$ ,  $[N]$  and  $[B]$  are defined in Equations (11, 8 and 10), substituting them into Equations (13.a and 13.b) we obtain:

$$[k_s]^e = [[A]^{-1}]^T \left( \int_0^{y_e} \int_0^{x_e} [Q]^T [P] [Q] dx dy \right) [A]^{-1} \quad (14.a)$$

$$[m_s]^e = \rho_s h [[A]^{-1}]^T \left( \int_0^{y_e} \int_0^{x_e} [R]^T [R] dx dy \right) [A]^{-1} \quad (14.b)$$

where  $x_e$  and  $y_e$  are dimensions of an element according to the  $X$  and  $Y$  coordinates, respectively. These integrals are calculated analytically using Maple mathematical software.

## 3 Fluid-solid interaction

The fluid pressure acting upon the structure is generally expressed as a function of out-of-plane displacement and its derivatives i.e. velocity and acceleration. These three terms are respectively known as the centrifugal, Coriolis and inertial forces [16]. The fluid matrices will be combined with solid matrices as follows:

$$\begin{aligned} & [[M_s] - [M_f]] \{\ddot{\delta}_T\} + [[C_s] - [C_f]] \{\dot{\delta}_T\} + \\ & [[K_s] - [K_f]] \{\delta_T\} = \{O\} \end{aligned} \quad (15)$$

where  $[M_s]$ ,  $[C_s]$  and  $[K_s]$  are the global matrices of mass, damping and rigidity of the elastic plate,  $[M_f]$ ,  $[C_f]$  and  $[K_f]$  represent the inertial, Coriolis and centrifugal forces of potential flow and  $\{\delta_T\}$  is the global displacement vector. The elementary matrices of solid are calculated in Equation (14).

### 3.1 Fluid-solid finite element

The fluid-solid model is developed based on the following hypotheses: (i) the fluid flow is potential; (ii) vibration is linear (small deformations); (iii) the fluid mean velocity distribution ( $U_x$ ) is constant

across a plate section and (iv) the fluid is incompressible.

Taking these assumptions into consideration, the velocity potential must satisfy the Laplace equation. This relation is expressed in the Cartesian system by:

$$\frac{\partial^2 \phi}{\partial x^2} + \frac{\partial^2 \phi}{\partial y^2} + \frac{\partial^2 \phi}{\partial z^2} = 0 \quad (16)$$

where  $\phi$  is the potential function. The Bernoulli equation is given by:

$$\frac{\partial \phi}{\partial t} + \frac{1}{2} V_r^2 + \frac{P}{\rho_f} \Big|_{z=0} = 0 \quad (17)$$

where  $P$  is the fluid pressure,  $V_r$  is the fluid velocity and  $\rho_f$  is the fluid density.

The components of fluid velocity along  $X, Y, Z$  directions, respectively are defined by:

$$V_x = U_x + \frac{\partial \phi}{\partial x} \quad V_y = \frac{\partial \phi}{\partial y} \quad V_z = \frac{\partial \phi}{\partial z} \quad (18)$$

where  $U_x$  is the mean velocity of fluid in the  $x$ -direction. Fig. 2 depicts a fluid-solid finite element subjected to flowing fluid on its upper surface.

Introducing Equation (18) into (17) and neglecting the non-linear terms we can write the dynamic pressure at the solid-fluid interface as follows (see Fig. 2):

$$P|_{z=0} = -\rho_f \left( \frac{\partial \phi}{\partial t} + U_x \frac{\partial \phi}{\partial x} \right) \Big|_{z=0} \quad (19)$$

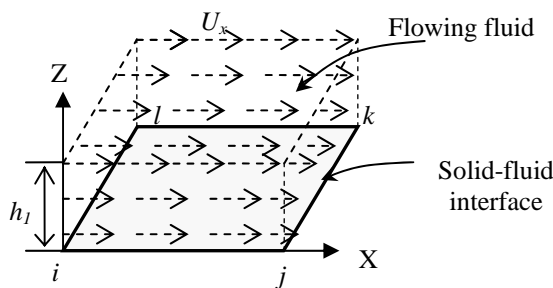


Fig. 2: Fluid-solid finite element

The impermeability condition ensures contact between the shell and the fluid. This should be:

$$\frac{\partial \phi}{\partial z} \Big|_{z=0} = \left( \frac{\partial W}{\partial t} + U_x \frac{\partial W}{\partial x} \right) \quad (20)$$

The following separate variable relation is assumed for the potential velocity function:

$$\phi(x, y, z, t) = F(z)S(x, y, t) \quad (21)$$

where  $F(z)$  and  $S(x, y, t)$  are two separate functions to be defined.

The following expression may be defined by introducing Equation (21) into (20)

$$S(x, y, t) = \frac{1}{dF(0)/dz} \left( \frac{\partial W}{\partial t} + U_x \frac{\partial W}{\partial x} \right) \quad (22)$$

For  $x$  and  $y$  in the finite element domain (see Fig. 2) the potential and pressure at the interface are coupled by the transverse movement of the plate  $W(x, y, t)$  and its derivatives. Equation (22) describes the function  $S(x, y, t)$  in terms of this transverse movement of the plate which itself varies as a function of plate geometry and time. Therefore, the movement of the fluid at any point on the interface (including the boundaries  $x$  and  $y$ ) is intimately linked to the movement of the edges of the structure. Then, substituting Equation (22) into (21), results in the following expression for the potential function:

$$\phi(x, y, z, t) = \frac{F(z)}{dF(0)/dz} \left( \frac{\partial W}{\partial t} + U_x \frac{\partial W}{\partial x} \right) \quad (23)$$

The only unknown function in Equation (22) is  $F(z)$ . By introducing Equation (23) into Equation (16), we obtain the following differential equation of second order:

$$\frac{d^2 F(z)}{dz^2} - \mu^2 F(z) = 0 \quad (24)$$

where:

$$\mu = \pi \sqrt{1/A^2 + 1/B^2}$$

The solution of this last equation is:

$$F(z) = A_1 e^{\mu z} + A_2 e^{-\mu z} \quad (25)$$

where  $A_1$  and  $A_2$  are unknown constants. By substituting Equation (25) into Equation (23) the potential function becomes:

$$\phi(x, y, z, t) = \frac{(A_1 e^{\mu z} + A_2 e^{-\mu z})}{dF(0)/dZ} \left( \frac{\partial W}{\partial t} + U_x \frac{\partial W}{\partial x} \right) \quad (26)$$

$A_1$  and  $A_2$  are two constants to be determined using the fluid boundary conditions. We note that at the solid-fluid interface ( $Z=0$ ) we have the impermeability condition (20) which is common for all cases. At the second limit of fluid ( $Z=h_1$ ), we have a boundary condition corresponding to either a rigid wall, an elastic plate or an infinite fluid level.

For each case we have a distinct solution. Below we will calculate the pressure of fluid acting on only one side ( $Z=h_1$ ) of the plate. If the fluid pressure acts on two sides, the total dynamic pressure will be a combination of the pressures corresponding to the fluid boundary conditions at both top and bottom ( $Z=h_2$ ) surfaces of the plate.

The presented approach may be adapted to model curved structures subjected to flowing fluid

such as turbine blades. To accomplish this the local matrices must be transformed to the global system before assembling into the global matrices [21].

**3.1.1 Fluid-solid finite element subject to flowing fluid with infinite level of fluid**

When the flowing fluid height on and/or under the plate ( $h_1$  and/or  $h_2$ ) is infinite (see Fig. 3), we assume that very far from the plate the potential is null. This boundary condition is written as follows:

$$\begin{aligned} \phi &= 0 \\ Z &\rightarrow \pm\infty \end{aligned} \quad (27)$$

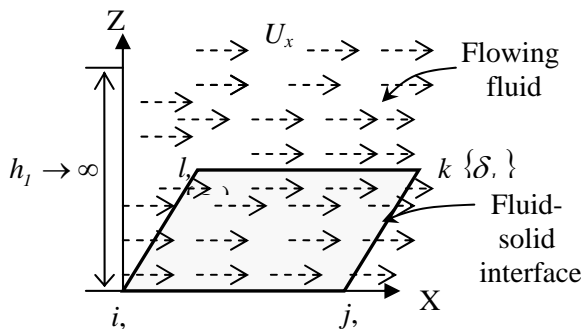


Fig. 3: Fluid-solid finite element subjected to flowing fluid with infinite height

In order to avoid an infinite potential, the constant  $A_1$  of Equation (26) must be null. Equation (20) permits us to calculate the second constant  $A_2$ . The potential expression becomes:

$$\phi(x,y,z,t) = -\frac{F'(0)e^{-\mu z}}{\mu} \left( \frac{\partial W}{\partial t} + U_x \frac{\partial W}{\partial x} \right) \quad (28)$$

The introduction of Equation (28) into relation (19), results in the following expression for the pressure function

$$P = \frac{\rho_f}{\mu} \left[ \frac{\partial^2 W}{\partial t^2} + 2U_x \frac{\partial^2 W}{\partial x \partial t} + U_x^2 \frac{\partial^2 W}{\partial x^2} \right] \quad (29)$$

or:

$$P = Z_{f1} \left[ \frac{\partial^2 W}{\partial t^2} + 2U_x \frac{\partial^2 W}{\partial x \partial t} + U_x^2 \frac{\partial^2 W}{\partial x^2} \right] \quad (30)$$

**3.1.2 Fluid-solid finite element subject to flowing fluid bounded by rigid wall**

As shown in Fig. 4, fluid flows between a rigid wall and an elastic plate. This provides another boundary condition at  $Z=h_1$  when the impermeability condition is taken into account. This boundary

condition is adopted by Lamb [11], McLachlan [12] and is expressed by:

$$\left. \frac{\partial \phi}{\partial z} \right|_{Z=h_1} = 0 \quad (31)$$

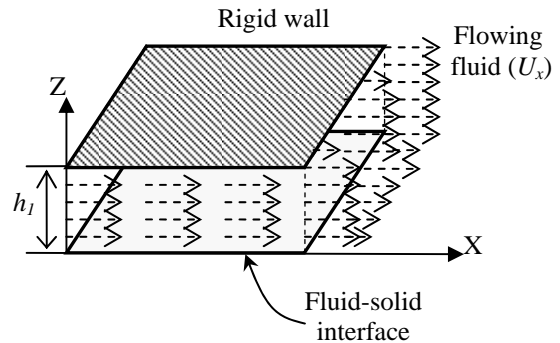


Fig. 4: Fluid solid finite element in contact with flowing fluid bounded by a rigid wall

Using Equations (20) and (31) we can calculate the constants  $A_1$  and  $A_2$  corresponding to this last boundary condition. Substituting these constants into (26) we obtain:

$$\begin{aligned} \phi(x,y,z,t) &= \frac{F'(0)}{\mu} \frac{(e^{-2\mu h_1} e^{\mu z} + e^{-\mu z})}{(e^{-2\mu h_1} - 1)} \times \\ &\left( \frac{\partial W}{\partial t} + U_x \frac{\partial W}{\partial x} \right) \end{aligned} \quad (32)$$

Replacing Equation (32) into (19), the corresponding dynamic pressure becomes:

$$P = -\frac{\rho_f (e^{-2\mu h_1} + 1)}{\mu (e^{-2\mu h_1} - 1)} \left[ \frac{\partial^2 W}{\partial t^2} + 2U_x \frac{\partial^2 W}{\partial x \partial t} + U_x^2 \frac{\partial^2 W}{\partial x^2} \right] \quad (33)$$

or:

$$P = Z_{f2} \left[ \frac{\partial^2 W}{\partial t^2} + 2U_x \frac{\partial^2 W}{\partial x \partial t} + U_x^2 \frac{\partial^2 W}{\partial x^2} \right] \quad (34)$$

**3.1.3 Fluid-solid finite element subject to flowing fluid bounded by elastic plate**

When fluid flows through two parallel elastic plates (see Fig. 5) two transverse vibration modes, in-phase and out-of-phase, should be considered. The impermeability condition at the solid-fluid interface remains the same for both modes while the boundary condition at  $Z=h_1$  changes according to the mode of vibration (in-phase or out-of-phase).

**3.1.3.1 In-phase mode**

In the case of the in-phase mode the boundary condition at fluid limits  $Z=h_1$  is expressed as follows [10]:

$$\left. \frac{\partial \phi}{\partial z} \right|_{z=h_1} = \left( \frac{\partial W}{\partial t} + U_x \frac{\partial W}{\partial x} \right) \quad (35)$$

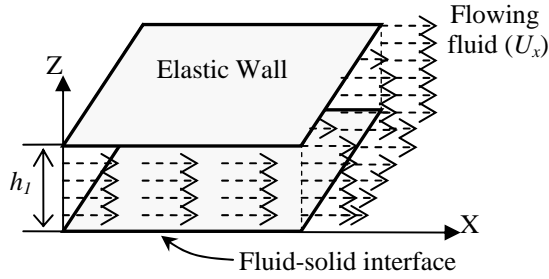


Fig. 5: Fluid-solid finite element in contact with flowing fluid bounded by an elastic plate

Similarly,  $A_1$  and  $A_2$  can be calculated by introducing Equation (26) into relations (20) and (35). The substitution of these constants in Equation (26) enables us to develop the following expression for the potential:

$$\phi(x, y, z, t) = \frac{1}{\mu} \left[ \frac{(1 - e^{-\mu h_1}) e^{\mu z} + (1 - e^{\mu h_1}) e^{-\mu z}}{e^{\mu h_1} - e^{-\mu h_1}} \right] \times \left( \frac{\partial W}{\partial t} + U_x \frac{\partial W}{\partial x} \right) \quad (36)$$

By replacing Equation (36) into (19) we obtain the following expression for pressure:

$$P = -\frac{\rho_f}{\mu} \left( \frac{2 - e^{-\mu h_1} - e^{\mu h_1}}{e^{\mu h_1} + e^{-\mu h_1}} \right) \times \left[ \frac{\partial^2 W}{\partial t^2} + 2U_x \frac{\partial^2 W}{\partial x \partial t} + U_x^2 \frac{\partial^2 W}{\partial x^2} \right] \quad (37)$$

or:

$$P = Z_{f3} \left[ \frac{\partial^2 W}{\partial t^2} + 2U_x \frac{\partial^2 W}{\partial x \partial t} + U_x^2 \frac{\partial^2 W}{\partial x^2} \right] \quad (38)$$

### 3.1.3.2 Out-of-phase mode

The boundary condition for the out-of-phase mode is expressed as follows [10]:

$$\left. \frac{\partial \phi}{\partial z} \right|_{z=\frac{h_1}{2}} = 0 \quad (39)$$

Here again,  $A_1$  and  $A_2$  can be calculated using Equations (26, 39 and 20). The potential function may be written as follows:

$$\phi(x, y, z, t) = \frac{F'(0)}{\mu} \frac{(e^{-\mu h_1} e^{\mu z} + e^{-\mu z})}{(e^{-\mu h_1} - 1)} \left( \frac{\partial W}{\partial t} + U_x \frac{\partial W}{\partial x} \right) \quad (40)$$

Using Equations (40) and (19) we obtain the following dynamic pressure:

$$P = -\frac{\rho_f (e^{-\mu h_1} + 1)}{\mu (e^{-\mu h_1} - 1)} \left[ \frac{\partial^2 W}{\partial t^2} + 2U_x \frac{\partial^2 W}{\partial x \partial t} + U_x^2 \frac{\partial^2 W}{\partial x^2} \right] \quad (41)$$

or:

$$P = Z_{f4} \left[ \frac{\partial^2 W}{\partial t^2} + 2U_x \frac{\partial^2 W}{\partial x \partial t} + U_x^2 \frac{\partial^2 W}{\partial x^2} \right] \quad (42)$$

## 3.2 Calculation of Fluid-Induced Force

The elementary vector of fluid-induced force is expressed by:

$$\{F\}^e = \int_A [N]^T \{P_v\} dS \quad (43)$$

where  $[N]$  is the shape function matrix of the finite element defined in Equation (8),  $\{P_v\}$  is a tensor expressing the pressure applied by the fluid on the plate and  $S$  is the elementary fluid-structure interface area.

By placing the matrix  $[N]$  of Equation (8) into Equation (43), the element load vector becomes:

$$\{F\}^e = \int_A [[A]^{-1}]^T [R]^T \{P_v\} dS \quad (44)$$

The dynamic pressures of Equations (29, 33, 37 and 41) may be rewritten as:

$$P = Z_{fi} \left[ \frac{\partial^2 W}{\partial t^2} + 2U_x \frac{\partial^2 W}{\partial x \partial t} + U_x^2 \frac{\partial^2 W}{\partial x^2} \right] \quad (45)$$

where  $Z_{fi}$  ( $i=1, 4$ ), depends on the boundary conditions (see Equations 30, 34, 38 and 42) and  $P$  is the only non-zero component in the pressure tensor  $\{P_v\}$ . Substituting Equation (2.c) into (45) the pressure expression becomes:

$$P = Z_{fi} \left[ \frac{\partial^2 W}{\partial t^2} + 2U_x \frac{i\pi}{A} \frac{\partial W}{\partial t} + U_x^2 \frac{i^2 \pi^2}{A^2} W \right] \quad (46)$$

The transversal displacement can be separated from Equation (8) as follows:

$$\begin{Bmatrix} 0 \\ 0 \\ W \end{Bmatrix} = [R_f][A]^{-1} \{\delta\} \quad (47)$$

where  $[R_f]$  is a (3x24) matrix given in the Appendix. Substituting Equation (47) into (46), we obtain the following expression for pressure:

$$\{P_v\} = Z_{fi} [R_f][A]^{-1} \left( \{\ddot{\delta}\} + 2U_x \frac{i\pi}{A} \{\dot{\delta}\} + U_x^2 \frac{i^2 \pi^2}{A^2} \{\delta\} \right) \quad (48)$$

By combining Equations (44) and (48) the element load vector is given by the following relation:

$$\{F\}^e = Z_{\beta} \left( \begin{array}{l} \int_A [[A]^{-1}]^T [R]^T [R_f] [A]^{-1} \{\ddot{\delta}\} dS + \\ 2U_x \frac{i\pi}{A} \int_A [[A]^{-1}]^T [R]^T [R_f] [A]^{-1} \{\dot{\delta}\} dS \\ + U_x^2 \frac{i^2 \pi^2}{A^2} \int_A [[A]^{-1}]^T [R]^T [R_f] [A]^{-1} \{\delta\} dS \end{array} \right) \quad (49)$$

Note that the force induced by a flowing fluid is a function of acceleration, velocity and displacement of the solid finite element. From Equation (49) we can separate the added matrices induced by flowing fluid, respectively describing inertial, Coriolis and centrifugal effects as follows:

$$[m_f]^e = Z_{\beta} \int_A [[A]^{-1}]^T [R]^T [R_f] [A]^{-1} dA \quad (50.a)$$

$$[c_f]^e = 2U_x Z_{\beta} \frac{i\pi}{A} \int_A [[A]^{-1}]^T [R]^T [R_f] [A]^{-1} dA \quad (50.b)$$

$$[k_f]^e = U_x^2 Z_{\beta} \left( \frac{i\pi}{A} \right)^2 \int_A [[A]^{-1}]^T [R]^T [R_f] [A]^{-1} dA \quad (50.c)$$

Dynamic equilibrium requires a combination of the last three elementary matrices with corresponding matrices given in Equation (14).

#### 4 Eigenvalue problem

A rectangular plate is subdivided into a series of quadrilateral finite elements such that each of them is a smaller rectangular plate (see Fig. 1.b). The positions of the nodal points of the elements are chosen in such a way that the local and global coordinates are parallel. An in-house computer code has been developed to establish the structural matrices of each element based on the equations developed using this theoretical approach. The global matrices mentioned in Equation (15) are obtained by superimposing the matrices for each individual element. After applying the boundary conditions these matrices are reduced to square matrices of order  $6*N-NC$ , where  $N$  is the number of nodes in the structure and  $NC$  is the number of constraints applied. The eigenvalue problem is solved by means of the equation reduction technique. Equation (15) may be rewritten as follows:

$$\begin{bmatrix} [0] & [M] \\ [M] & [C] \end{bmatrix} \begin{Bmatrix} \{\ddot{\delta}_T\} \\ \{\dot{\delta}_T\} \end{Bmatrix} + \begin{bmatrix} -[M] & [0] \\ [0] & [K] \end{bmatrix} \begin{Bmatrix} \{\delta_T\} \\ \{\delta_T\} \end{Bmatrix} = \{0\} \quad (51)$$

where:

$[M] = [M_s] - [M_f]$ ,  $[C] = [C_f]$ ,  $[K] = [K_s] - [K_f]$ ,  $\{\delta_T\}$  is the global displacement vector and structural damping is neglected. The eigenvalue problem is given by:

$$[[DD] - \lambda[I] = 0 \quad (52)$$

where :

$[[DD] = \begin{bmatrix} 0 & [I] \\ [K]^{-1}[M] & [K]^{-1}[C] \end{bmatrix}$ ,  $\lambda = 1/i\omega^2$  and  $[I]$  is the identity matrix.

#### 5 Results and discussions

The precision of the finite element method depends on the number of elements used to discretize the physical problem. The first set of calculations is therefore to determine the requisite number of elements for a precise determination of the natural frequencies.

The variation of the first five frequencies versus the number of finite elements of rectangular plate simply supported on its four sides is plotted in Fig. 6 and shows the minimum required number of elements to assure fast convergence in determining both low and high frequencies. The values of the material and geometrical properties used in the calculations are: Young's modulus  $E=196\text{GPa}$ , material density  $\rho=7860 \text{ kg/m}^3$ , Poisson's ratio  $\nu=0.3$ , thickness  $h=2.54 \text{ mm}$ ,  $A=609.6 \text{ mm}$  and  $B=304.8\text{mm}$ .

Eight elements are sufficient to calculate the two first modes, whereas for other modes convergence requires at least twenty five elements. This number of elements required by the present method is much lower than that of other existing approaches. In all of the following examples 64 elements are used, which assures that the results will be independent of mesh size.

In order to show that the developed model provides accurate results, calculations were performed on the same plate used in the convergence test. The first six natural frequencies are listed in Table 1 along with analytical results and ANSYS output data. It can be seen that the present method gives fairly good results compared to the exact solution and the commercial finite element code

An extensive study has been conducted to test the solid finite element in vacuum in reference [7]. Free vibrations of rectangular plates were obtained for a variety of boundary conditions and plate dimension ratios ( $A/B$ ). The computed natural













